

Supplementary Tables, Figures and References

High-throughput screening of soybean di-nitrogen fixation and seed nitrogen content using spectral sensing

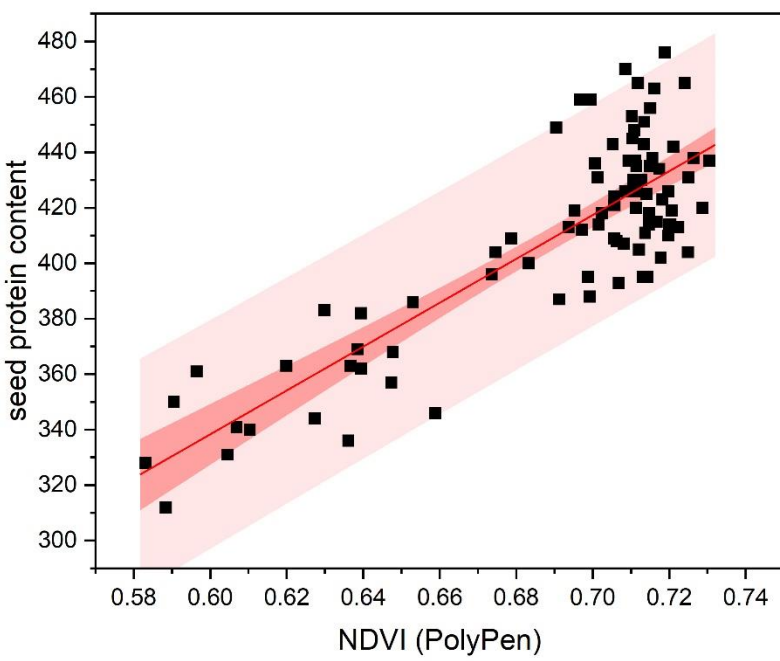
J. Vollmann, P. Rischbeck, M. Pachner, V. Đorđević, A.M. Manschadi

Suppl. Table 1

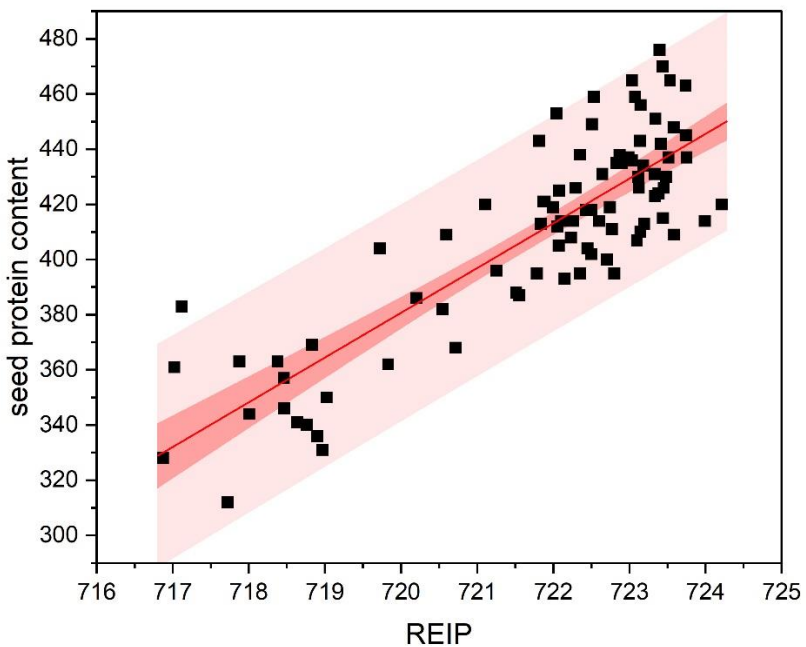
Descriptive list of spectral reflectance indices (SRI) calculated with wavepoints utilized and reference to formulae and full description.

Index	Description of index	Wavepoints used (nm)	Reference used
NDVI	NDVI, normalized difference vegetation index (biomass, yield, leaf area)	670, 800	Jansen et al 2014
SIPI	SIPI, structure insensitive pigment index (carotenoid / chlorophyll a ratio)	455, 680, 800	Jansen et al 2014
PSSRa	PSSRa, pigment specific simple ratio (chlorophyll a)	680, 800	Jansen et al 2014
PSSRb	PSSRb (chlorophyll b)	635, 800	Jansen et al 2014
CRI	CRI 1 , carotenoids reflectance index (carotenoid content)	510, 550	Jansen et al 2014
ARI	ARI 1, anthocyanin reflectance index (anthocyanin content)	550, 700	Jansen et al 2014
PSSRc	Pigment-specific simple ratio (carotenoid content)	470, 800	Mahlein et al 2019
NRI	Nitrogen reflectance index	570, 670	Cao et al 2015
RVSI	Red-edge vegetation stress index	712, 732, 752	Cao et al 2015
PSRI	Plant senescence reflectance index	500, 680, 750	Cao et al 2015
CI	CI red edge; Canopy chlorophyll and nitrogen content (red edge chlorophyll index)	710, 780	Chen et al 2019
PRI570	PRI=phytochemical reflectance index; plant water status	531, 569	Rossini 2013
DCNI	Double-peak canopy nitrogen index	670, 700, 720	Duan et al 2019
GI	Greenness index (chlorophyll)	554, 677	Duan et al 2019
GNDVI	Green normalized difference vegetation index	550, 750	Duan et al 2019
VOG1	Vogelmann index 1	720, 740	Inostroza et al 2016
VOG2	Vogelmann index 2	715, 726, 734, 747	Inostroza et al 2016
VOG3	Vogelmann index 3	710, 715, 734, 747	Inostroza et al 2016
R705	Blue nitrogen index (leaf nitrogen content); R705/(R717+R491)	705, 717, 491	Tian et al 2010, cited according to Feng et al 2016
R780/740	Total N uptake	740, 780	Prey et al 2020
MSR705_445	Modified simple ratio 705/445	705, 445	Prey et al 2020
REIP	Red edge inflection point (nitrogen content)	670, 700, 740, 780	Prey et al 2020
WI	WI, reflectance water index (water content)	900, 970	Prey et al 2020

NWI-1	Norm. water index 1	900, 970	Prey et al 2020
NWI-2	Norm. water index 2	850, 970	Prey et al 2020
NWI-3	Norm. water index 3	920, 970	Prey et al 2020
NWI-4	Norm. water index 4	880, 970	Prey et al 2020
NWI-5	Norm. water index 5	930, 970	Prey et al 2020
WI_1	Water index 1 (soybean)	915, 940	Christenson et al 2016
WI_2	Water index 2 (soybean)	915, 990	Christenson et al 2016
WI_3	Water index 3 (soybean)	940, 990	Christenson et al 2016
RNDVI_1	red NDVI 1	680, 915	Christenson et al 2016
RNDVI_2	red NDVI 2	680, 940	Christenson et al 2016
RNDVI_3	red NDVI 3	680, 990	Christenson et al 2016
RENDVI_1	red edge NDVI 1	715, 915	Christenson et al 2016
RENDVI_2	red edge NDVI 2	715, 940	Christenson et al 2016
RENDVI_3	red edge NDVI 3	715, 990 670, 800, 900, 970	Christenson et al 2016 Ihuoma 2019
WI / NDVI	WI : NDVI	970	Ihuoma 2019
WBI	Water band index (1/WI)	900, 970	Lausch et al 2015
MA1_N	R5 NDVI normalized diff vegetation index 638_674	638, 674	Zhang et al 2019
MA1_R	R5 RVI Ratio vegetation index 638_674 (optimized for soybean at R5)	638, 674	Zhang et al 2019
MB1_N	R5 NDVI normalized diff vegetation index 634_678	634, 678	Zhang et al 2019
MB1_R	R5 RVI Ratio vegetation index 634_678	634, 678	Zhang et al 2019



a



b

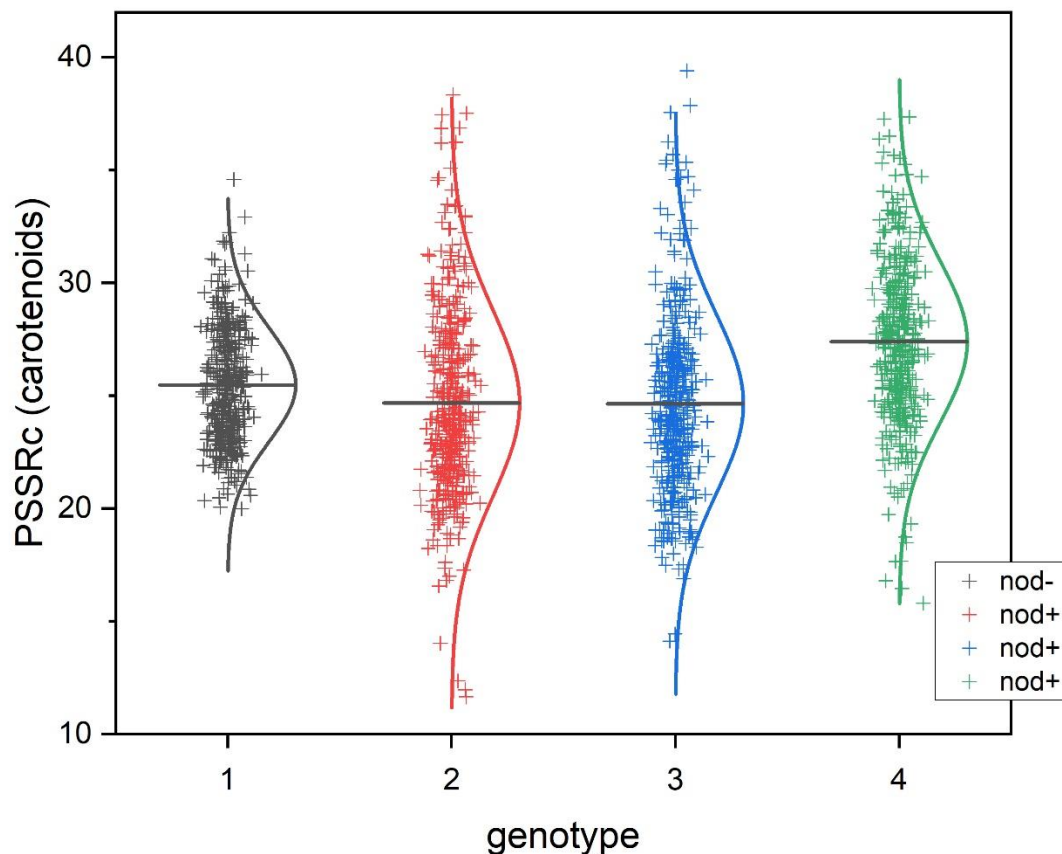
Suppl. Fig. 1. Scatter plots illustrating relationships between either NDVI index (Polypen RP410 NIR measurement; $r=0.836$; $n=88$) (a) or REIP index (ASD FieldSpec Handheld2 measurement; $r=0.920$; $n=88$) (b) taken at R3-4 stage (28 Jul 2020) and seed protein content (TU 2020).

Suppl. Table 2

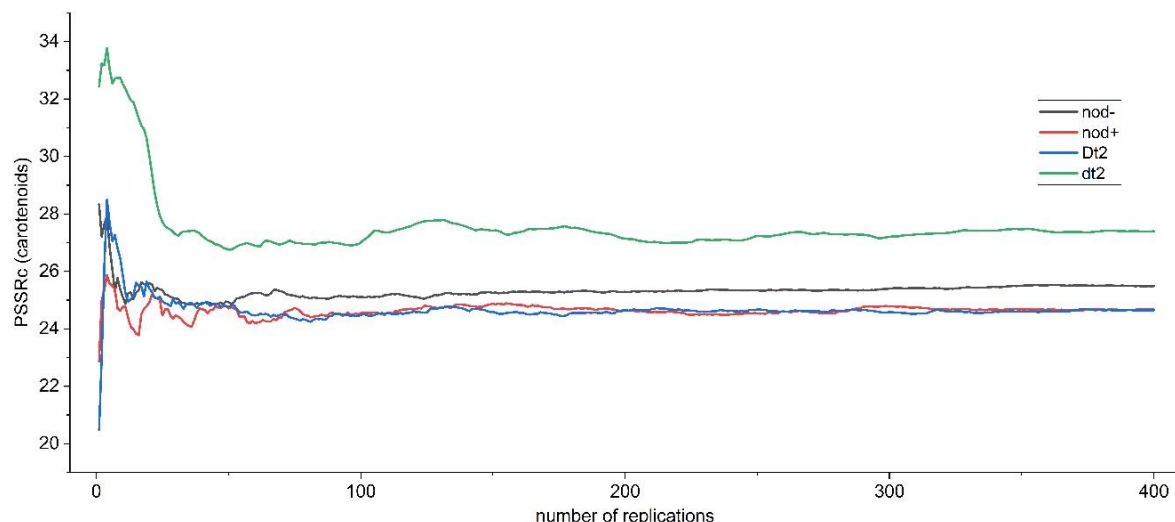
Comparative ANOVA results (data: standardization through z-transformation) for spectral reflectance indices (SRIs) derived from Polypen RP410 NIR measurements, phenotypic measurements, and ASD FieldSpec Handheld2 indices determined at TU 2020 plots.

	parameter	Model F ratio	Genotype F ratio	Error mean square
SRIs by Polypen PR 410	NDVI	16.017	15.939	0.077
	SR	15.367	15.225	0.08
	OSAVI	5.565	5.688	0.216
	ZMI	27.911	27.935	0.045
	Ctr2	16.762	16.723	0.074
	Lic1	3.463	3.451	0.338
	GM2	22.066	21.971	0.056
Phenotypic data	RDVI	6.842	7.075	0.177
	Time to maturity	14.17	14.384	0.087
	Plant height	6.462	6.639	0.187
	Oil content	8.893	8.837	0.137
	Protein content	17.941	17.964	0.069
	Sucrose content	12.493	12.405	0.099
SRIs by ASD Handheld2	1000-seed weight	12.028	12.311	0.102
	NDVI	11.542	11.65	0.107
SRIs by ASD Handheld2	SIPI	8.367	8.487	0.146
	PSSRa	7.904	7.97	0.154
	PSSRb	13.876	13.965	0.089
	CRI	12.146	12.375	0.101
	ARI	8.893	9.205	0.137
	PSSRc	4.419	4.541	0.269
	NRI	6.128	6.36	0.197
	RVSI	1.124	1.174	0.91
	PSRI	16.471	16.639	0.075
	CI	19.385	19.377	0.064
	PRI570	15.806	15.992	0.078
	DCNI	14.249	14.759	0.087
	GI	5.207	5.415	0.23
	GNDVI	26.865	27.211	0.046
	VOG1	21.57	21.476	0.058
	VOG2	18.774	18.576	0.066
	VOG3	17.921	17.753	0.069
	R705	32.253	32.644	0.039
MSR705_445	R780_740	13.802	13.724	0.089
	REIP	22.058	22.091	0.056
SRIs by ASD Handheld2	WI	27.058	27.134	0.046
	NWI_1	5.768	5.236	0.209
	NWI_2	5.693	5.163	0.211
	NWI_3	5.905	5.336	0.204
	NWI_4	4.587	4.21	0.26
	NWI_5	4.941	4.486	0.242
	WI_1	1.926	1.753	0.576
	WI_2	1.898	1.695	0.583
	WI_3	4.957	4.497	0.241
	RNDVI_1	1.397	1.392	0.76

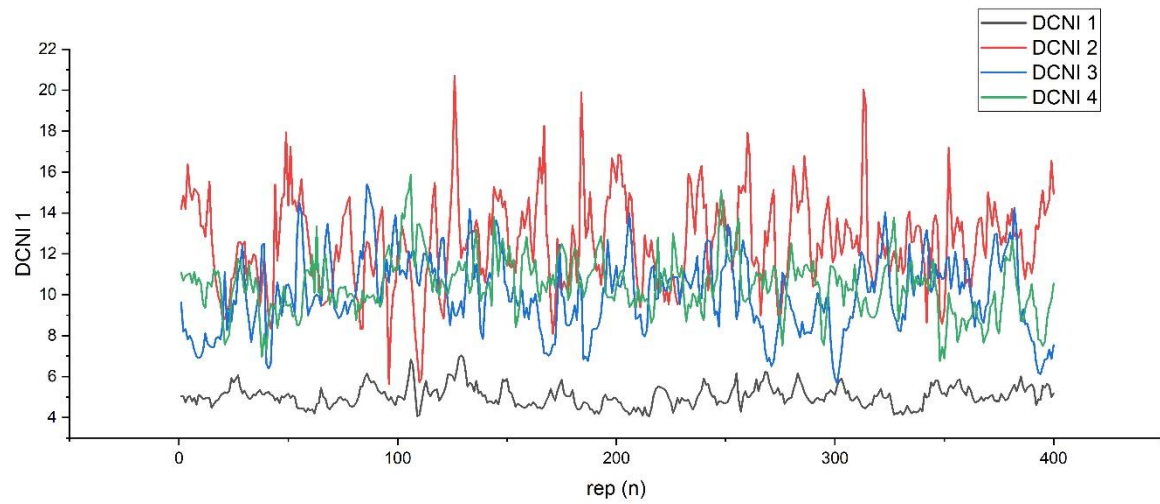
RNDVI_2	9.555	9.742	0.128
RNDVI_3	10.805	11.002	0.114
RENDVI_1	21.584	21.855	0.058
RENDVI_2	21.266	21.672	0.058
RENDVI_3	25.07	25.531	0.05
WI_NDVI	5.454	5.453	0.22
WBI	5.625	5.096	0.214
MA1_N	26.663	27.328	0.047
MA1_R	25.05	25.674	0.05
MB1_N	25.699	26.323	0.048
MB1_R	24.284	24.881	0.051



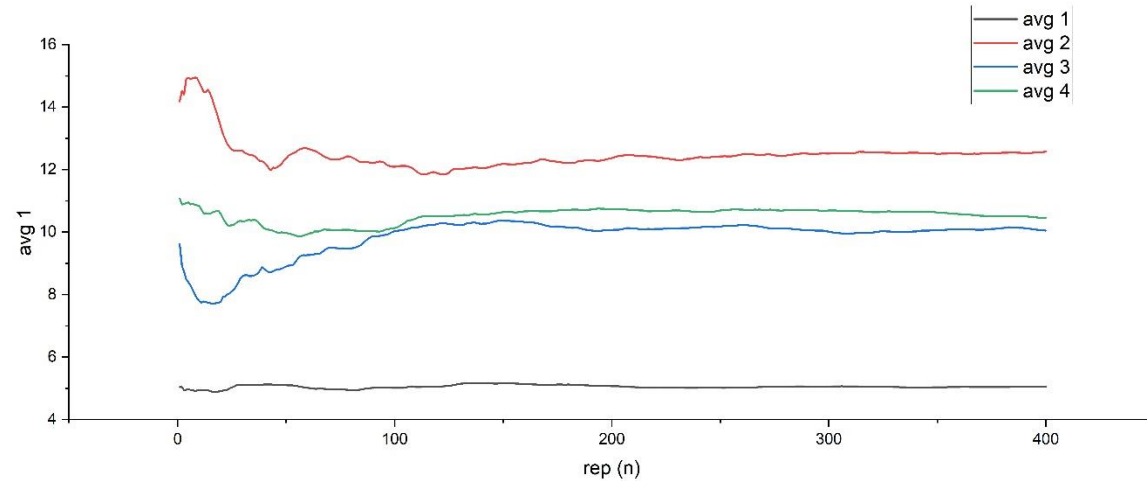
Suppl. Fig. 2. Index PSSRc indicating carotenoid content of 4 genotypes differing in nodulation status (1=non-nodulating, 2, 3, 4: nodulating) measured in a total of 400 replications.



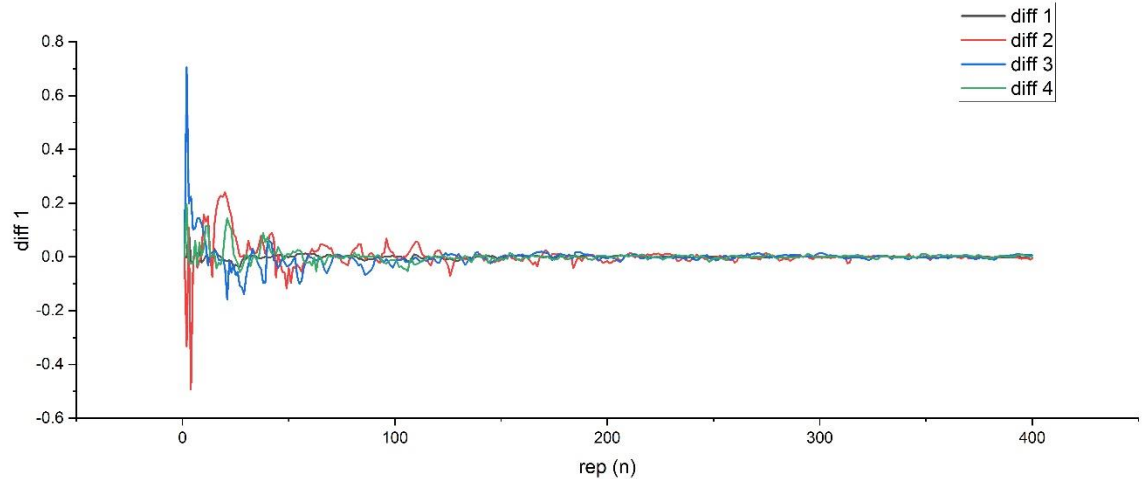
Suppl. Fig. 3. Effect of the number of replications for measuring carotenoids (PSSR c) in 4 genotypes differing in nodulation status.



a

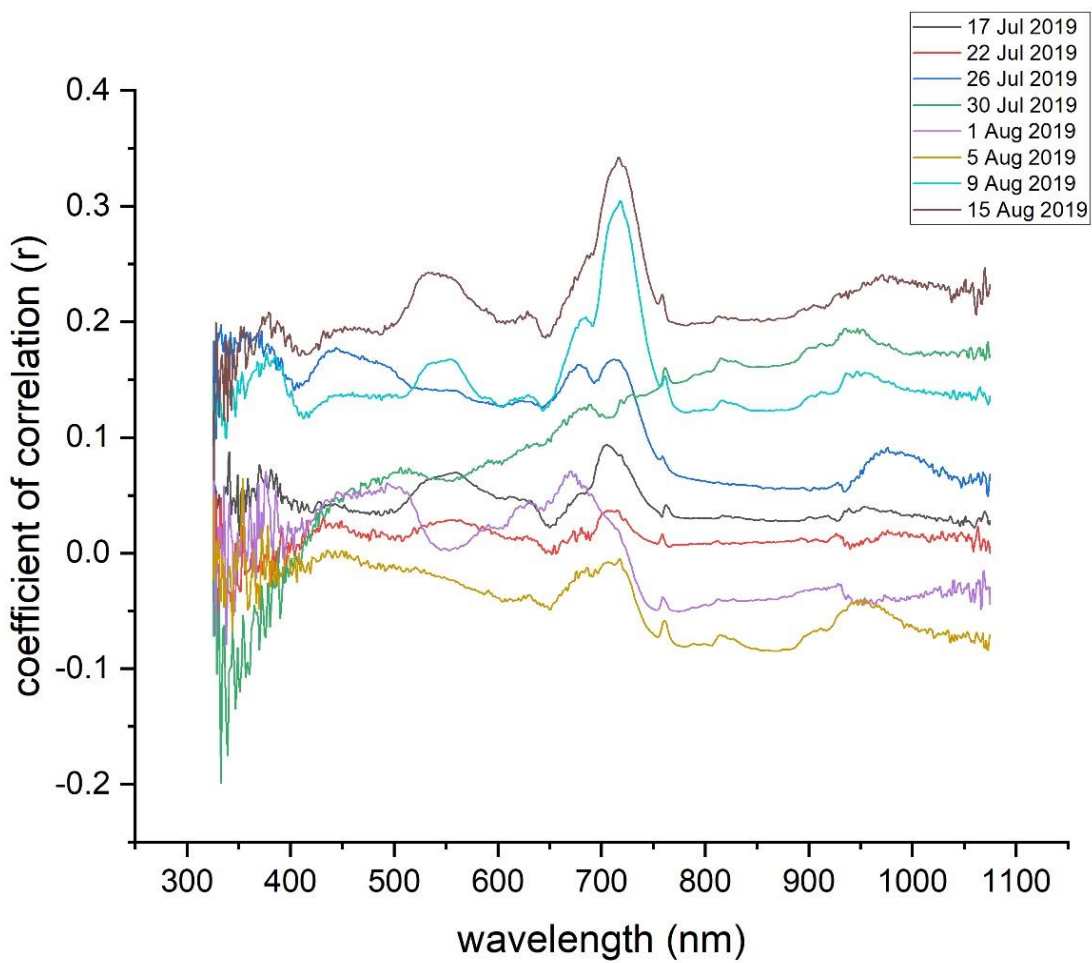


b

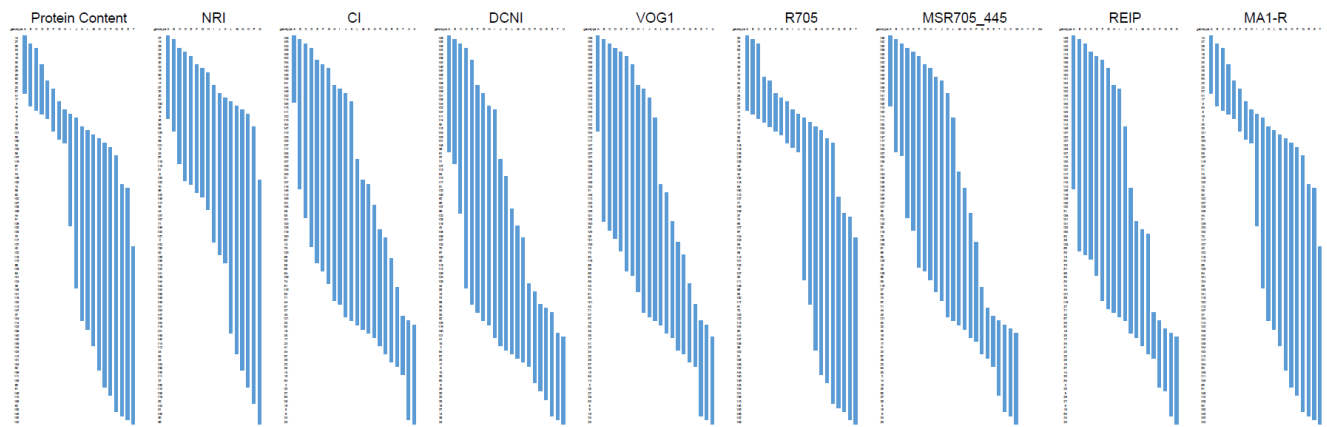


c

Suppl. Fig. 4. Double-peak canopy nitrogen index (DCNI) measured in 400 spectral replications for 4 different genotypes (1: non-nodulating; 2, 3, 4: nodulating). Individual DCNI values (a), DCNI averages across replications (b), differences to previous mean values from averaging across 1 to 400 replications (c).



Suppl. Fig. 5. Correlation between hyperspectral reflection at eight different data collection dates during the soybean seed filling period and seed protein content of the harvest product: Correlograms describing correlations between reflectance at given wavelengths (1 nm increment) and seed protein content for the Tulln 2019 subsets c, d and e (high seed protein selections, high pod set selections, and standards).

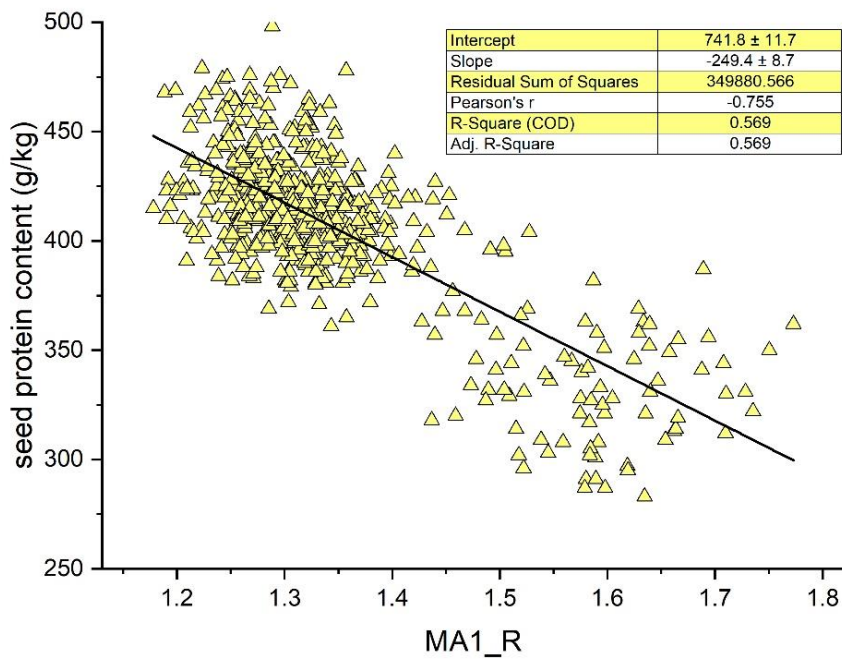


Suppl. Fig. 6. Tukey-Kramer mean separation (multiple comparison at $p=0.05$ level) of 94 soybean genotypes across 3 environments for seed protein content and 8 SRIs correlated to seed protein content.

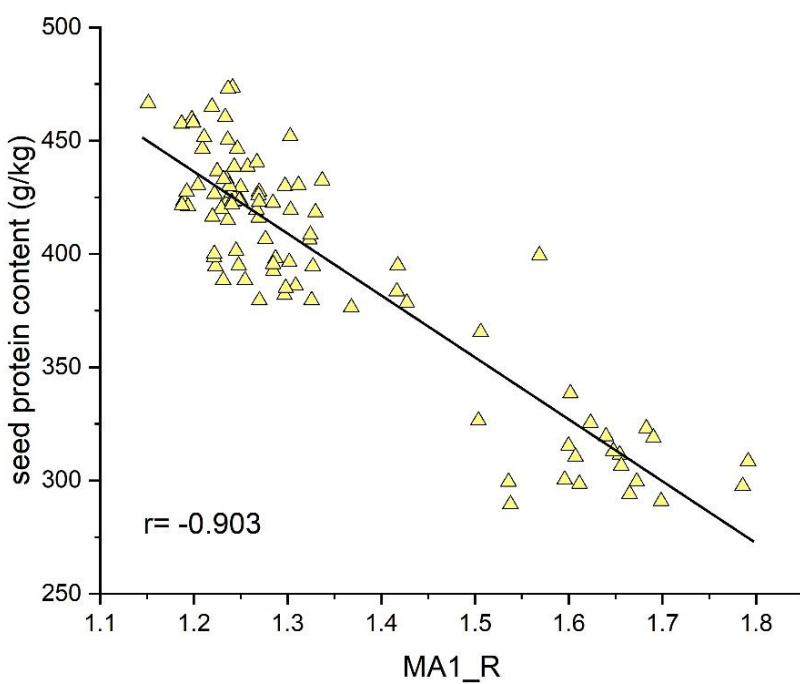
Suppl. Table 3

Pearson coefficients of correlation between soybean phenotypic traits and SRIs (n=630, individual plots basis, 3 environments; highest correlations indicated by yellow background).

INDEX	mat	p_height	oil	prot	sucr	tsw	INDEX
NDVI	0.282	0.368	-0.349	0.347	-0.182	0.357	NDVI
SIP1	0.258	0.335	-0.238	0.221	-0.111	0.264	SIP1
PSSRa	0.263	0.338	-0.338	0.327	-0.196	0.356	PSSRa
PSSRb	0.235	0.308	-0.504	0.534	-0.377	0.476	PSSRb
CRI	-0.146	-0.131	-0.218	0.287	-0.339	0.185	CRI
ARI	-0.061	-0.034	-0.443	0.517	-0.482	0.368	ARI
PSSRc	0.204	0.262	-0.062	0.028	-0.013	0.115	PSSRc
NRI	0.071	0.053	0.510	-0.612	0.529	-0.365	NRI
RVSI	0.301	0.246	-0.457	0.402	-0.328	0.377	RVSI
PSRI	-0.286	-0.359	0.446	-0.439	0.198	-0.429	PSRI
CI	0.285	0.359	-0.607	0.623	-0.433	0.545	CI
PRI570	0.403	0.440	-0.609	0.617	-0.375	0.571	PRI570
DCNI	-0.004	0.046	-0.561	0.639	-0.539	0.467	DCNI
GI	0.099	0.078	0.485	-0.590	0.518	-0.336	GI
GNDVI	0.201	0.297	-0.568	0.618	-0.431	0.503	GNDVI
VOG1	0.318	0.392	-0.623	0.631	-0.423	0.559	VOG1
VOG2	-0.381	-0.437	0.634	-0.622	0.407	-0.569	VOG2
VOG3	-0.356	-0.411	0.628	-0.621	0.417	-0.565	VOG3
R705	-0.105	-0.207	0.580	-0.659	0.471	-0.507	R705
R780/740	0.395	0.463	-0.600	0.585	-0.385	0.534	R780/740
MSR705_445	0.248	0.311	-0.627	0.654	-0.459	0.560	MSR705_445
REIP	0.310	0.405	-0.620	0.640	-0.428	0.545	REIP
WI	0.554	0.623	-0.421	0.290	-0.089	0.408	WI
NWI-1	-0.554	-0.623	0.422	-0.290	0.089	-0.408	NWI-1
NWI-2	-0.567	-0.618	0.460	-0.334	0.109	-0.455	NWI-2
NWI-3	-0.534	-0.634	0.391	-0.256	0.068	-0.378	NWI-3
NWI-4	-0.570	-0.621	0.436	-0.312	0.096	-0.433	NWI-4
NWI-5	-0.433	-0.520	0.265	-0.150	0.041	-0.287	NWI-5
WI_1	-0.383	-0.345	0.327	-0.301	0.126	-0.321	WI_1
WI_2	-0.486	-0.606	0.386	-0.233	0.063	-0.353	WI_2
WI_3	-0.187	-0.329	0.134	-0.007	-0.030	-0.106	WI_3
RNDVI_1	0.256	0.343	-0.321	0.322	-0.175	0.332	RNDVI_1
RNDVI_2	0.238	0.329	-0.308	0.311	-0.171	0.320	RNDVI_2
RNDVI_3	0.227	0.308	-0.302	0.316	-0.178	0.317	RNDVI_3
RENDVI_1	0.275	0.375	-0.586	0.610	-0.416	0.519	RENDVI_1
RENDVI_2	0.255	0.360	-0.579	0.606	-0.419	0.511	RENDVI_2
RENDVI_3	0.240	0.332	-0.579	0.620	-0.434	0.512	RENDVI_3
WI / NDVI	0.234	0.205	-0.028	-0.100	0.114	0.006	WI / NDVI
WBI	-0.553	-0.623	0.422	-0.291	0.089	-0.409	WBI
MA1_N	-0.066	-0.120	0.645	-0.751	0.585	-0.520	MA1_N
MA1_R	-0.059	-0.121	0.646	-0.755	0.586	-0.521	MA1_R
MB1_N	-0.056	-0.124	0.631	-0.739	0.578	-0.511	MB1_N
MB1_R	-0.050	-0.125	0.634	-0.745	0.580	-0.513	MB1_R

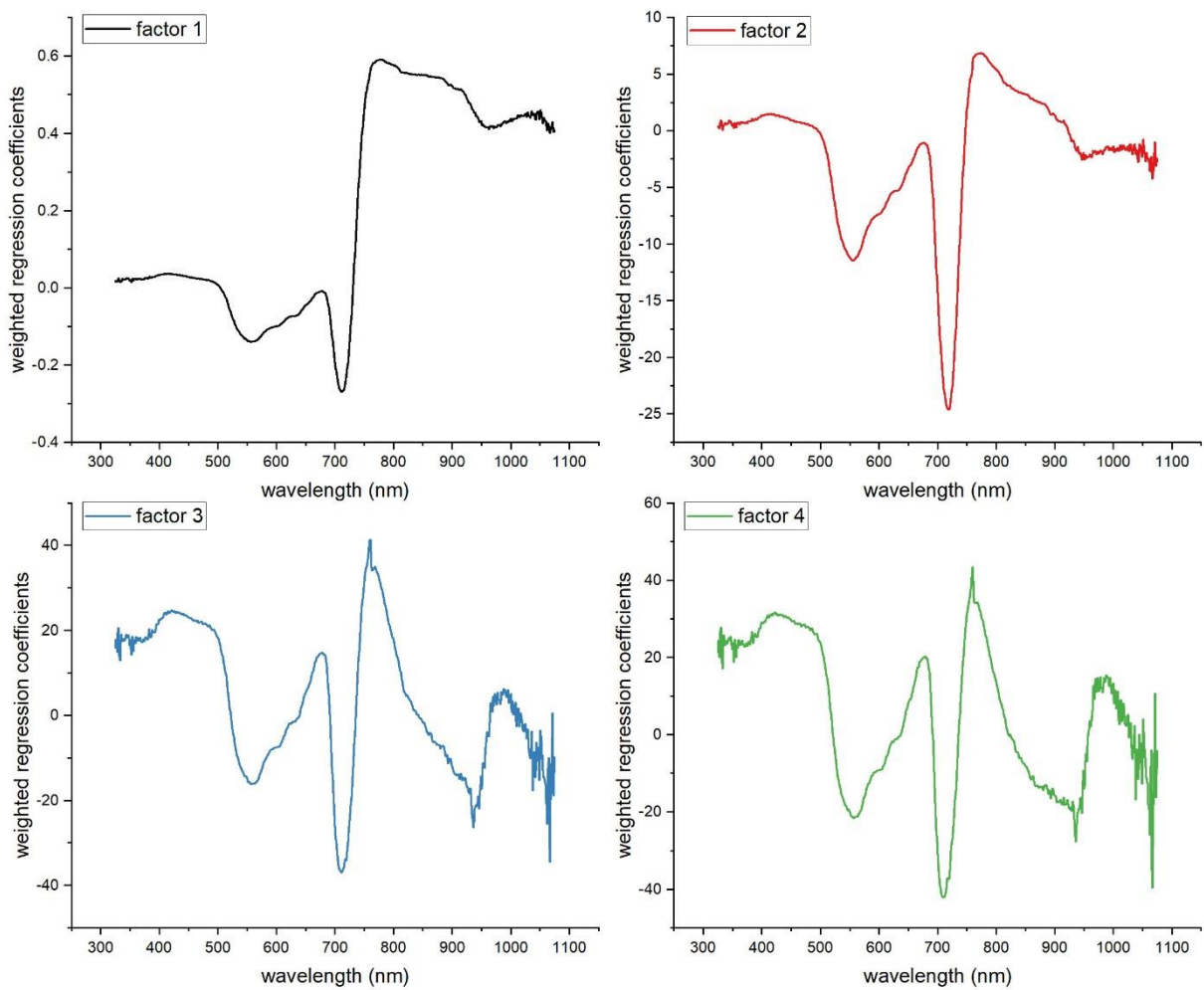


a

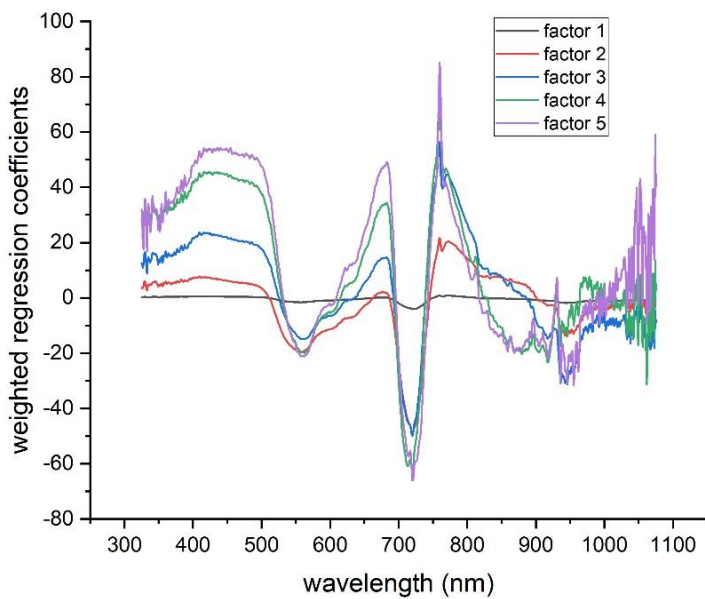


b

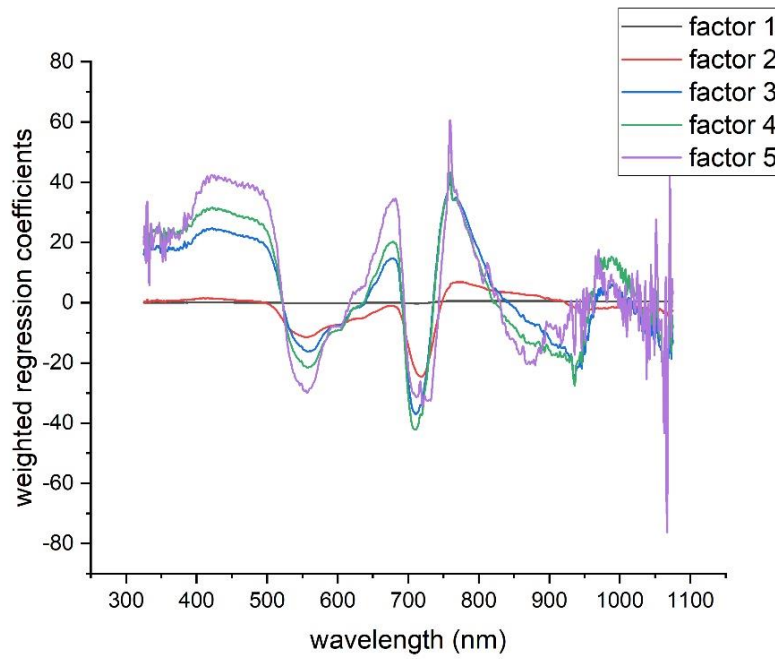
Suppl. Fig. 7. Correlation between index MA1_R and seed protein content; a: individual plot basis (all plots in all environments), b: genotype LSMEANS basis (means of TU 2019 experiment only).



Suppl. Fig. 8. Weighted regression coefficients for four main PLS regression factors across the total wavelength range utilized (model across all three environments).



a



b

Suppl. Fig. 9. Weighted regression coefficients for most important PLS regression factors across the whole wavelength range; a: for the TU 2019 model, b: for the model across all environments.

References to Suppl. Table 1

- Cao X., Luo Y., Zhou Y., Fan J., Xu X., West J.S., Duan X., Cheng D. 2015. Detection of powdery mildew in two winter wheat plant densities and prediction of grain yield using canopy hyperspectral reflectance. PLOS ONE. DOI: 10.1371/journal.pone.0121462.
- Chen J., Li F., Wang R., Fan Y., Raza M.A., Liu Q., Wang Z., Cheng Y., Wu X., Yang F., Yang W. 2019. Estimation of nitrogen and carbon content from soybean leaf reflectance spectra using wavelet analysis under shade stress. Computers and Electronics in Agriculture 156, 482-489. DOI: 10.1016/j.compag.2018.12.003.
- Christenson B.S., Schapaugh Jr. W.T., An N., Price K.P., Prasad V., Fritz A.K. 2016. Predicting soybean relative maturity and seed yield using canopy reflectance. Crop Sci. 56, 625–643. DOI: 10.2135/cropsci2015.04.0237.
- Duan D.D., Zhao C.J., Li Z.H., Yang G.J., Zhao Y., Qiao X.J., Zhang Y.H., Zhang L.X., Yang W.D. 2019. Estimating total leaf nitrogen concentration in winter wheat by canopy hyperspectral data and nitrogen vertical distribution. J. Integr. Agricul. 18, 1562-1570. DOI: 10.1016/S2095-3119(19)62686-9.
- Feng W., Zhang H.Y., Zhang Y.S., Qi S.L., Heng Y.R., Guo B.B., Ma D.Y., Guo T.C. 2016. Remote detection of canopy leaf nitrogen concentration in winter wheat by using water resistance vegetation indices from in-situ hyperspectral data. Field Crops Res. 198, 238-246. DOI: 10.1016/j.fcr.2016.08.023.
- Ihuoma S.O., Madramootoo C.A. 2019. Sensitivity of spectral vegetation indices for monitoring water stress in tomato plants. Computers and Electronics in Agriculture 163. DOI: 10.1016/j.compag.2019.104860.
- Inostroza L., Acuña H., Munoz P., Vásquez C., Ibáñez J., Tapia G., Pino M.T., Aguilera H. 2016. Using aerial images and canopy spectral reflectance for high-throughput phenotyping of white clover. Crop Sci. 56, 2629-2637. DOI: 10.2135/cropsci2016.03.0156.
- Jansen M., Bergsträsser S., Schmittgen S., Müller-Linow M., Rascher U. 2014. Non-invasive spectral phenotyping methods can improve and accelerate cercospora disease scoring in sugar beet breeding. Agriculture 4, 147-158. DOI: 10.3390/agriculture4020147.
- Lausch A., Salbach C., Schmidt A., Doktor D., Merbach I., Pause M. 2015. Deriving phenology of barley with imaging hyperspectral remote sensing. Ecol. Model. 295, 123-135. DOI: 10.1016/j.ecolmodel.2014.10.001.
- Mahlein, A.K., Alisaac, E., Al Masri, A., Behmann, J., Dehne, H.W., Oerke, E.C. 2019. Comparison and combination of thermal, fluorescence, and hyperspectral imaging for monitoring Fusarium head blight of wheat on spikelet scale. Sensors 19, 2281. DOI: 10.3390/s19102281.
- Prey L., Hu Y., Schmidhalter U. 2020. High-throughput field phenotyping traits of grain yield formation and nitrogen use efficiency: optimizing the selection of vegetation indices and growth stages. Front. Plant Sci. 10, 1672. DOI: 10.3389/fpls.2019.01672.
- Rossini M., Fava F., Cogliati S., Meroni M., Marchesi A., Panigada C., Giardino C., Busetto L., Migliavacca M., Amaducci S., Colombo R. 2013. Assessing canopy PRI from airborne imagery to map water stress in maize. ISPRS J. Photogr. Remote Sens. 86, 168–177. DOI: 10.1016/j.isprsjprs.2013.10.002.
- Zhang X., Zhao J., Yang G., Liu J., Cao J., Li C., Zhao X., Gai J. 2019. Establishment of plot-yield prediction models in soybean breeding programs using UAV-based hyperspectral remote sensing. Remote Sens. 11, 2752. DOI: 10.3390/rs11232752.